



HAL
open science

Terahertz beats of vibrational modes studied by femtosecond coherent Raman spectroscopy

R. Leonhardt, W. Holzapfel, W. Zinth, W. Kaiser

► **To cite this version:**

R. Leonhardt, W. Holzapfel, W. Zinth, W. Kaiser. Terahertz beats of vibrational modes studied by femtosecond coherent Raman spectroscopy. *Revue de Physique Appliquée*, 1987, 22 (12), pp.1735-1741. 10.1051/rphysap:0198700220120173500 . jpa-00245733

HAL Id: jpa-00245733

<https://hal.science/jpa-00245733>

Submitted on 4 Feb 2008

HAL is a multi-disciplinary open access archive for the deposit and dissemination of scientific research documents, whether they are published or not. The documents may come from teaching and research institutions in France or abroad, or from public or private research centers.

L'archive ouverte pluridisciplinaire **HAL**, est destinée au dépôt et à la diffusion de documents scientifiques de niveau recherche, publiés ou non, émanant des établissements d'enseignement et de recherche français ou étrangers, des laboratoires publics ou privés.

Classification
 Physics Abstracts
 42.65 — 32.50

Terahertz beats of vibrational modes studied by femtosecond coherent Raman spectroscopy

R. Leonhardt, W. Holzappel, W. Zinth and W. Kaiser

Physik Department Ell der Technischen Universität München, München, F.R.G.

(Reçu le 9 juin 1987, accepté le 18 septembre 1987)

Résumé. — Une technique par Raman cohérent femtoseconde récemment développée permet de mesurer des spectres Raman cohérent à transformée de Fourier avec des différences haute-fréquence. L'excitation simultanée de différents modes de vibration avec une force motrice accordable à large bande conduit à un fort battement de la diffusion Raman cohérent de la sonde. La haute résolution temporelle du montage expérimental permet de mesurer des battements de fréquence de plus de 10 THz avec une précision élevée.

Abstract. — A recently developed femtosecond coherent Raman technique allows the measurement of Fourier transform coherent Raman spectra with high-frequency differences. The simultaneous excitation of different vibrational modes with a broad-band tunable driving force leads to a strong beating of the coherent Raman probe scattering. The high time resolution of the experimental set-up allows one to measure beat frequencies of more than 10 THz with high precision.

1. Introduction.

During the past decade, time-resolved coherent Raman methods have attracted considerable interest for the study of fast dynamic processes. In particular, time-resolved coherent Raman scattering made it possible to measure — in the time domain — rapid dephasing processes of molecular vibrations in liquids and elucidated various line broadening mechanisms [1-5]. It is the aim of this paper to focus attention on a more recent application. Although time-resolved Raman scattering collects data in the time domain, it allows valuable information to be obtained in the frequency domain. There are various approaches to relate the time and the frequency domain [6-11]: (i) Time resolved coherent Raman scattering, where the spectrum of the coherently scattered light is recorded, has been extensively studied using picosecond light pulses. It is possible to remove the homogeneous contribution to the transition line-width. One finds spectra with narrower lines and one obtains transition frequencies with high accuracy. This technique has been applied to the study of congested spectral regions, where the spontaneous Raman spectrum is smooth, but where the line-narrowing technique revealed structure due to distinct transitions [9-11]. (ii) In the second method the time evolution of the coherent Raman probe signal is recorded with high time resolution.

The Fourier transformation of the experimental data gives a difference frequency spectrum. The frequency resolution of this technique can be improved by using numerical filtering procedures prior to the Fourier transformation. (iii) A third way to analyse the data is a comparison of the data taken in a high time resolution experiment with time dependent functions. High accuracy can be obtained for the determination of difference frequencies.

In this letter we present new experimental data of time-resolved coherent Raman spectroscopy taken with a novel femtosecond Raman spectrometer [12, 13]. The results of these time-domain experiments are subsequently numerically analysed. In this way we obtain frequency differences with high precision. The high time resolution of the femtosecond coherent Raman set-up allows one to measure very high difference frequencies. After a short theoretical description of the basic ideas of the technique we give experimental results. We show that terahertz quantum beats up to 10 THz can be measured giving precise values for the frequency differences of vibrational transitions separated by up to 350 cm^{-1} .

2. Theory.

Time-resolved coherent Raman scattering is commonly treated under the following assumptions [1]. The light fields are described by Maxwell's equation

and the vibrational transitions are represented by two-level systems. Changes in the population of the two molecular levels are neglected (weak Raman interaction). The expectation value of the vibrational amplitude, the coherent amplitude $\langle q \rangle$, is the relevant quantity for the description of time-resolved coherent Raman spectroscopy. First, we discuss the coherent experiment for a single homogeneously broadened transition with dephasing time T_2 . We use the ansatz of plane waves for the coherent amplitude $\langle q \rangle = (i/2) Q \exp(-i\omega_q t + ik_q x) + \text{c.c.}$ and assume an isotropic Raman tensor for the investigated vibration. The coherent amplitude of a Raman active mode at frequency ω_q is excited *via* transient stimulated Raman scattering by a pair of light pulses, the laser pulse E_L and the Stokes pulse E_S [1, 14]. The electric fields are considered to be plane waves, e.g.

$$E_L = 1/2 E_L \exp(-i\omega_L t + ik_L x) + \text{c.c.}$$

with the wave vector k_L and frequency ω_L for the laser field. The driving force $F(x, t)$ for the coherent amplitude Q is proportional to the product of the laser and the Stokes field, $F(x, t) \propto E_L E_S^*$; as a result the frequency of the excitation force is $\omega_L - \omega_S$. The linear response theory applied to the excitation process leads to the following equation for the coherent amplitude Q :

$$Q(t) = \kappa \int_{-\infty}^t dt' E_L(t') E_S^*(t') \times \exp[(t' - t)/T_2 - i\Delta\omega t']. \quad (1)$$

The constant κ contains material parameters such as Raman cross-section and vibrational frequency ω_q (see Ref. [1]). T_2 stands for the dephasing time of the transition. Detuning between the excitation frequency and the vibrational mode is given by $\Delta\omega = \omega_L - \omega_S - \omega_q$. Under the action of a short exciting force the coherent amplitude $\langle q \rangle$ evolves as follows: $\langle q \rangle$ rises to a maximum with the exciting force and, subsequently, decays exponentially with the dephasing time T_2 . During the free exponential decay the molecules oscillate at the resonance frequency ω_q . In the experiment described here the large bandwidth of the short driving force allows several vibrations to be excited simultaneously. Since the excitation *via* stimulated Raman interaction is weak, the various modes evolve in time independent of each other. The different vibrations may be treated with the same ansatz introducing the individual resonance frequencies ω_{qj} , phase factors ϕ_j , amplitudes Q_j , and dephasing times T_{2j} .

In the time-resolved coherent Raman experiments, the amplitude $\langle q \rangle$ generated at time zero is monitored by coherent Raman scattering of a delayed probing pulse E_{L2} . We investigate light on

the anti-Stokes side of the Raman spectrum generated by the nonlinear polarization P_{AS}^{NL} :

$$P_{AS}^{NL} = \lambda \langle q \rangle E_{L2} + \chi_{NR}^{(3)} E_L E_S^* E_{L2}. \quad (2)$$

The coherent signal consists of two contributions. The first part on the r.h.s. of equation (2) describes the coherent Raman signal of interest scattered from the excited vibrational mode. The constant λ contains the Raman cross-section of the mode. This part of the coherent signal is emitted at the resonant anti-Stokes frequency $\omega_{AS} = \omega_{L2} + \omega_q$ and provides information on the dynamic properties of the investigated mode. The second part on the r.h.s. of equation (2) is related to the nonresonant nonlinear susceptibility $\chi_{NL}^{(3)}$ resulting from electronic contributions [15]. The nonresonant part of the signal gives an instantaneous response, i.e. it follows the product $E_L E_S^* E_{L2}$ and decays very rapidly with the time resolution of the experiment. The resonant part, on the other hand, shows the slow response of the resonantly excited vibrations. The nonresonant part of the coherent signal does not provide any information on the investigated modes. It has to be separated from the resonant signal. This fact is not possible in the steady-state coherent anti-Stokes Raman spectroscopy (CARS). In the time-resolved coherent anti-Stokes experiments described here the separation is possible due to the different time dependence of the two contributions: the rapidly decaying nonresonant part shows up around time zero, while at later delay times valuable information on the slower resonant part of the signal is collected.

In the present coherent experiment we measure the scattered Raman light as a function of the time delay t_D between excitation and probing pulses. In order to have optimum temporal resolution, pulses of very short duration for the exciting and probing laser fields are required.

Under these conditions the nonresonant signal is concentrated only around time zero and may be neglected at later times. Experimentally, one detects the time-integrated coherent signal $S(t_D)$:

$$\begin{aligned} S(t_D) &\propto \int_{-\infty}^{+\infty} dt |E_{AS}(t, t_D)|^2 \\ &\propto \int_{-\infty}^{+\infty} dt |P_{AS}^{NL}(t, t_D)|^2 \\ &\simeq \int_{-\infty}^{+\infty} dt |\lambda \langle q \rangle E_{L2}|^2. \end{aligned} \quad (3)$$

According to equation (3) one measures the time dependence of the coherent amplitude or — more exactly — one determines the absolute square of the coherent amplitude, which decays exponentially with $T_2/2$.

When several modes are excited simultaneously, the signal decay is more complex. It can be shown

that for very short driving and probing pulses the coherent signal is equivalent to the absolute square of the Fourier transform of the spontaneous Raman spectrum [6, 7]. Here we analyse the coherent Raman signal at late delay times, where the different vibrational modes oscillate at their resonance frequencies ω_{qj} and the amplitudes decay exponentially with the individual dephasing times T_{2j} . The coherent anti-Stokes field is the sum of the light field generated by the individual molecular modes Q_j . For short light pulses of duration $t_p \ll T_2$, $t_p \ll 1/\Delta\omega_{ij}$ one obtains :

$$E_{AS}(t, t_D) = \sum_j E_{ASj}(t, t_D) \propto \sum_j Q_j(t_D) \exp(-i\omega_j t_D). \quad (4)$$

According to equations (3) and (4) simultaneously excited modes lead to a beating of the coherent signal at the frequency differences $\Delta\omega_{ij}$ between the various transition frequencies $\Delta\omega_{ij} = \omega_i - \omega_j$. These « quantum beats » of the coherent signal may give accurate information on the vibrational spectrum.

The effect of different parameters on the coherent signal is readily seen for the simple example of two vibrational modes. We assume that the two modes with a frequency difference $\Delta\omega$ and dephasing times T_{21} and T_{22} are excited to the coherent amplitude Q_{j0} . For equal amplitudes $Q_{10} = Q_{20}$ one obtains for the coherent signal

$$S(t_D) = \left| \sum_{j=1,2} Q_{j0} \exp(-t_D/T_{2j} - i\omega_j t_D) \right|^2 = Q_{10}^2 [\exp(-2t_D/T_{21}) + \exp(-2t_D/T_{22}) + 2 \cos(\Delta\omega t_D) \exp(-t_D(T_{22} + T_{21})/T_{21} T_{22})] \quad (5)$$

The signal consists of the two contributions of the individual transitions decaying with the respective dephasing times (first two expressions on the r.h.s. of Eq. (5)). The interference between the two molecular modes gives rise to the third term of equation (5), which causes strong modulation of the signal. When the two dephasing times strongly differ, the modulation depth of the signal decreases with increasing time. At late delay times the modulation dies out and a single unmodulated exponential decay appears. As an example, the signal curve for two vibrational modes at $\Delta\omega = 10^{13} \text{ s}^{-1}$ ($= 53 \text{ cm}^{-1}$), $T_{21} = 6 \text{ ps}$ and $T_{22} = 2 \text{ ps}$, and $Q_1(0)/Q_2(0) = 0.9$ is depicted in figure 1. At early times, when the two coherent amplitudes $Q_1(t)$ and $Q_2(t)$ are not yet affected by the exponential decay, the signal is strongly modulated by the frequency difference $\Delta\omega$. At later times the more rapidly

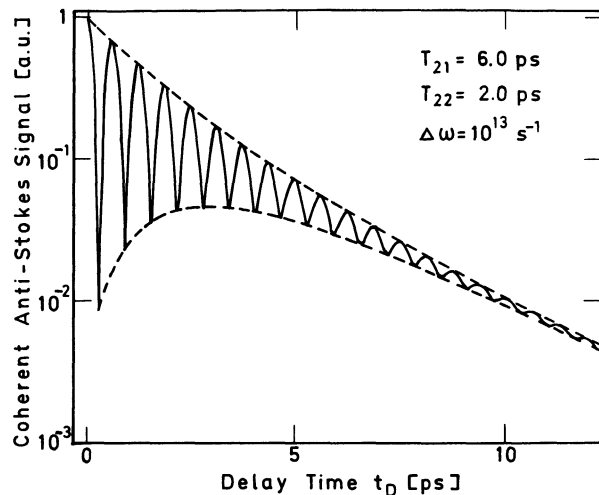


Fig. 1. — Coherent Raman signal calculated for two simultaneously excited molecular modes with the frequency difference $\Delta\omega = 10^{13} \text{ s}^{-1}$ ($\Delta = 53 \text{ cm}^{-1}$). The initial amplitudes have a ratio of $Q_{10}/Q_{20} = 0.9$ and dephasing times $T_{21} = 6 \text{ ps}$ and $T_{22} = 2 \text{ ps}$. The modulation of the signal decreases with the shorter one of the two dephasing times.

decaying coherent amplitude, and with it the modulation, vanishes. Data similar to figure 1 allow the determination of the two dephasing times and the frequency difference $\Delta\omega$.

For more complicated situations equations (3) and (4) permit the numerical analysis of the experimental data. With a least square-fit procedure one may deduce the molecular parameters such as dephasing times and frequency differences, by minimizing the difference between the experimental data and the theoretical curves. As shown below, the molecular quantities may be determined with high precision.

An alternative possibility to obtain the frequency-domain information from the time domain data is the straight forward application of a Fourier transformation [7]. As discussed in the literature it is advantageous to multiply the experimental data by a correction function, which compensates the exponential decay of the signal within the boundaries of the experimental time range. In this way the calculated line shape is not Lorentzian, and the accuracy of the line positions is improved.

3. Experimental.

The experimental system is depicted schematically in figure 2. Pulses from a mode-locked argon-ion laser synchronously pump two dye lasers. The specially designed femtosecond unidirectional ring (UDR) dye laser [16, 17] contains an amplifying jet (dye Rhodamine 6G) and an absorber jet (dye DODCI). The laser emits pulses with a duration of 80 fs at $\lambda = 625 \text{ nm}$ with an average power of 30 mW. The pulses from this laser provide us with the exciting

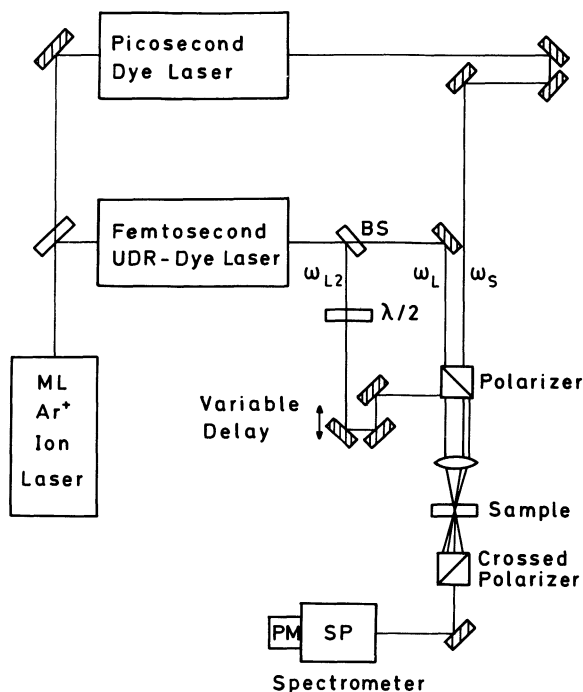


Fig. 2. — Experimental set-up used for Fourier transform coherent Raman spectroscopy. A mode-locked argon-ion laser synchronously pumps a femtosecond unidirectional ring dye laser (frequency ω_L) and a tunable picosecond dye laser (frequency ω_S). Excitation is done with a synchronized pair of pulses at ω_L and ω_S , while the probing pulses at ω_{L2} are produced by a beam splitter BS from the femtosecond laser pulses ω_L . The coherent anti-Stokes light generated *via* the probing pulse is recorded as a function of the time delay adjusted by the variable delay line.

pulses E_L and, *via* the beam splitter BS, with the probing pulses E_{L2} . The second laser is a standard synchronously mode-locked picosecond dye laser with amplifying dyes DCM or Pyridine 2 and a three-plate birefringent filter as a tuning element (power 30 mW). When tuned through the red and the infrared part of the spectrum, pulses E_S at the Stokes frequency ω_S of 6 ps duration are generated. The femtosecond pulses from the UDR laser and the picosecond pulses of the second laser, both with parallel polarization, serve to excite molecular vibrations with a tuning range between 300 cm^{-1} and $3\,000\text{ cm}^{-1}$. It can be derived from equation (1) that the driving force exists only for the time duration of the shorter of the two pulses, i.e. for a time of 80 fs. A major advantage of the system is the wide tunability of the excitation frequency $\omega_L - \omega_S$ with the help of the birefringent filter of the picosecond laser while keeping the favorable femtosecond time resolution. The coherent vibrational excitation is monitored by probing pulses derived from the femtosecond laser. These pulses are polarized perpendicular to the excitation pulses. The three beams are focused into the sample using a geometry appro-

priate for anti-Stokes phase matching. The anti-Stokes radiation E_{AS} generated by the probing process passes the second polarizer and is detected in conjunction with the broad-band spectrometer SP by the cooled photomultiplier PM. The coherent signal is recorded as a function of the delay time (set by the variable delay line) between the exciting and probing pulses.

4. Fourier transform coherent Raman spectroscopy of transitions with terahertz frequency differences.

High-resolution Fourier transform coherent Raman spectroscopy was first reported by Graener and Laubereau [7], who worked with light pulses of 20 ps duration. The authors studied vibrational-rotational transitions in CH_4 separated by less than 1 cm^{-1} with high frequency resolution of 10^{-3} cm^{-1} . The data were taken over a time interval of 12 ns. In the experiment described here we extend Fourier transform coherent Raman spectroscopy for the first time to the study of large frequency differences up to 350 cm^{-1} . To see the related beating phenomena one requires high time resolution. For example, a frequency difference of 350 cm^{-1} produces a beating pattern with peaks separated by 95 fs. In order to resolve this very rapid phenomenon, one has to work with femtosecond light pulses. Synchronized light pulses of approximately 80 fs duration became available only recently [16, 17] permitting the experiments reported here.

The first investigation treats vibrations in neat pyridine and in pyridine/cyclohexane mixtures. We study Raman active vibrations of liquid pyridine at frequencies 991 cm^{-1} and $1\,030\text{ cm}^{-1}$ assigned to two A_1 ring modes [18]. Both vibrations have similar spectral width ($\sim 2.2\text{ cm}^{-1}$) and similar Raman cross-sections; they are separated by 39 cm^{-1} . In the Raman excitation process a frequency difference of $(\omega_L - \omega_S)/2\pi c = 1\,010\text{ cm}^{-1}$ between the laser and the Stokes frequency is applied. Due to the broad spectral width of the femtosecond exciting force of more than 200 cm^{-1} both pyridine modes are simultaneously excited in the experiment. Figure 3a shows the observed anti-Stokes signal plotted as a function of the time delay between exciting and probing pulses. During the excitation process at time zero the coherent signal rises to a pronounced peak. It subsequently decays quickly over more than one order of magnitude. Later on the signal recovers and shows strong oscillations. The modulation depths exceeds a factor of ten. Two features of the coherent signal are of special interest here: (i) the period of oscillation is approximately 0.85 ps. Consequently, the frequency difference between the two modes is 1.18 THz. (ii) The peaks of the oscillation decay exponentially with the decay time $T_2/2 = 2.55 \pm 0.15\text{ ps}$. The depth of the oscilla-

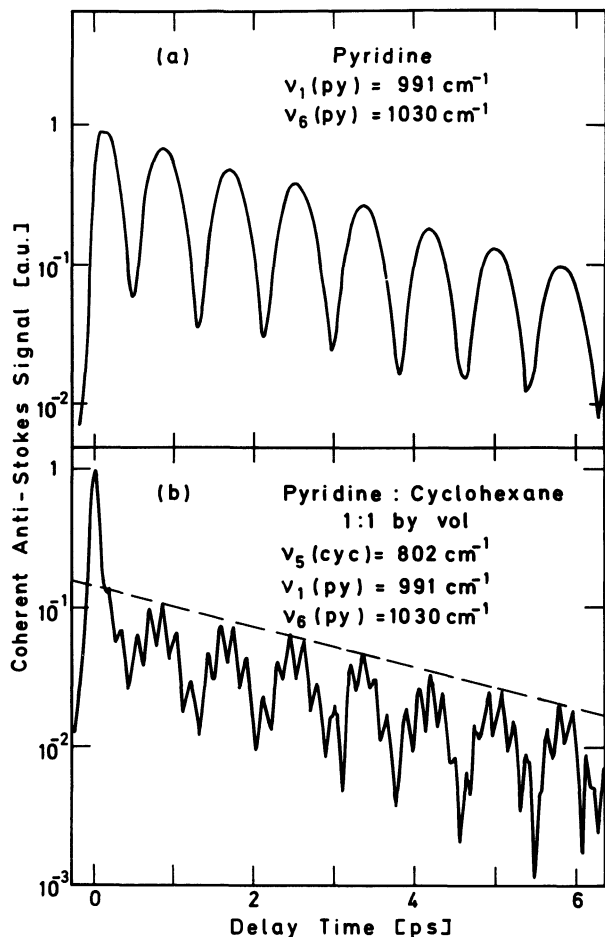


Fig. 3. — Time resolved coherent Raman scattering using femtosecond time resolution. (a) Beat pattern of pure pyridine after excitation of the two pyridine modes at 991 cm^{-1} and 1030 cm^{-1} . (b) Beat pattern of a mixture of pyridine and cyclohexane. Three molecular modes are excited.

tion slightly decreases for long observation times indicating a difference between the dephasing times of the two modes of 10 %.

In figure 3b we present an amazingly complicated, but perfectly reproducible anti-Stokes pattern. A mixture of cyclohexane and pyridine (1 : 1 by volume) was investigated with femtosecond light pulses. In this case three vibrational modes with similar T_2 values beat together. They are: one cyclohexane mode at 802 cm^{-1} [19] and two pyridine modes at 991 cm^{-1} and 1030 cm^{-1} . We find a rich beating structure originating from the interference of the three modes. The frequency differences of the excited modes are determined by the following procedure. The exponential decay is removed by multiplying the signal with an exponential rising function. An appropriate window function is introduced to remove the influence of the boundaries of the time range. After these arithmetical manipulations a Fourier transformation of the time-dependent data gives the results shown in figure 4. Three

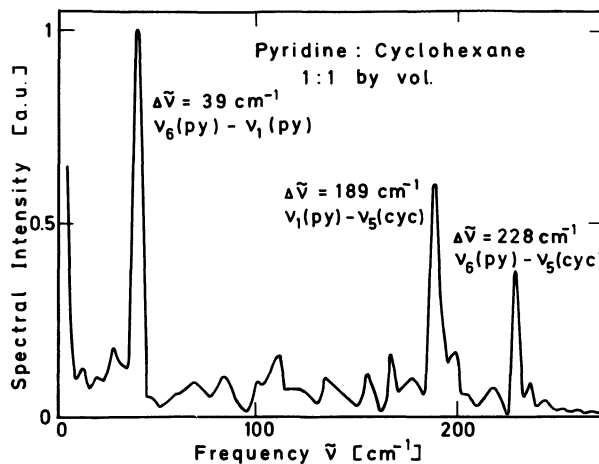


Fig. 4. — Difference spectrum of pyridine and cyclohexane obtained by numerical Fourier transformation of the time resolved data from figure 3b. Note the strong peaks at 39 cm^{-1} , 189 cm^{-1} , and 228 cm^{-1} , which correspond to the differences between the three excited modes. The highest difference frequency is $\Delta\nu = 6.84\text{ THz}$.

sharp and pronounced peaks are found at 39 cm^{-1} , 189 cm^{-1} and 228 cm^{-1} , which correspond to the frequency differences between the three modes excited in the mixture. The frequency width of the three different lines is approximately 5 cm^{-1} ; this width is due to the limited time range of observation (e.g. 6 ps in Fig. 3). The background noise in figure 4 reflects the experimental noise of figure 3 and the applied window function.

A very promising method to evaluate the experimental data is the modelling of the beat pattern according to equations (3) and (4). An example is given in figure 5a, where we consider two modes to simulate an extended beating pattern of neat pyridine (redrawn in Fig. 5b for ready comparison). Two theoretical curves are calculated for the same set of experimental parameters. Only the difference frequency $\Delta\omega$ was changed by the small amount of 0.4 cm^{-1} (i.e. 1 %) from 39.2 cm^{-1} (broken curve) to 39.6 cm^{-1} (solid curve). Superposition of the experimental and calculated curves gives an impressive fit over the entire time range. It is possible to deduce a very precise frequency difference of $39.4 \pm 0.2\text{ cm}^{-1}$.

Interesting results were obtained in the coherent Raman study of liquid nitrobenzene, where we observe the highest beat frequencies. With an excitation frequency at 1200 cm^{-1} we detect a rich beating structure. In figure 6b the coherent signal curve is plotted on a linear scale for a time interval from 0.2 ps to 2.5 ps. An extremely rapid modulation is found with the shortest time between subsequent peaks of less than 100 fs. A Fourier transform to the frequency domain reveals four strong peaks at 16 cm^{-1} , 104 cm^{-1} , 237 cm^{-1} , and 341 cm^{-1} , and a

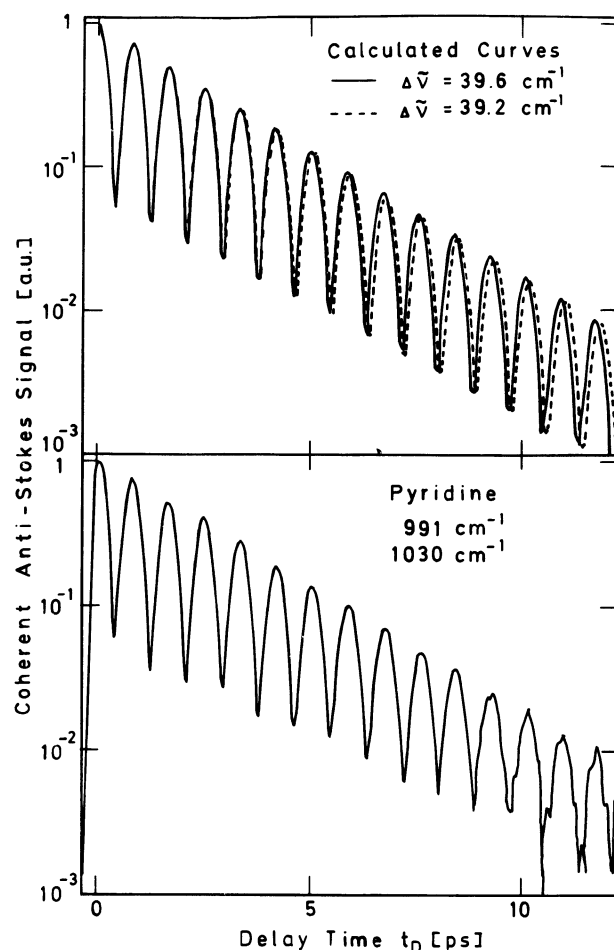


Fig. 5. — Time resolved coherent Raman data for liquid pyridine. (a) Two curves calculated according to equations (3) and (4) using the dephasing times T_{21} (991 cm^{-1}) = 5.1 ps and T_{22} (1030 cm^{-1}) = 4.7 ps and the frequency differences of 39.6 cm^{-1} and 39.2 cm^{-1} . Comparison of the calculated curves with the experimental data of figure 5b gives a very accurate number for the frequency difference between the two modes of $\Delta\nu = 39.4 \pm 0.2 \text{ cm}^{-1}$.

number of weaker peaks. The value of 341 cm^{-1} or 10.5 THz corresponds to the beating of the two nitrobenzene modes at 1000 cm^{-1} and 1341 cm^{-1} . Both modes were excited simultaneously in the transient stimulated Raman process. In figure 6a we show a beat curve calculated for the following set of data :

$$\begin{aligned} \nu/c &= 1000 \text{ cm}^{-1}, & T_2 &= 2.9 \text{ ps} \\ &1016.4 \text{ cm}^{-1}, & T_2 &= 2.7 \text{ ps} \\ &1104.2 \text{ cm}^{-1}, & T_2 &= 1.1 \text{ ps} \\ &1340.9 \text{ cm}^{-1}, & T_2 &= 2.1 \text{ ps} \end{aligned}$$

Using a least square-fit procedure to adjust the theoretical parameters a very good agreement of the theoretical and experimental curves is achieved. The data analysing procedure indicates that the frequency

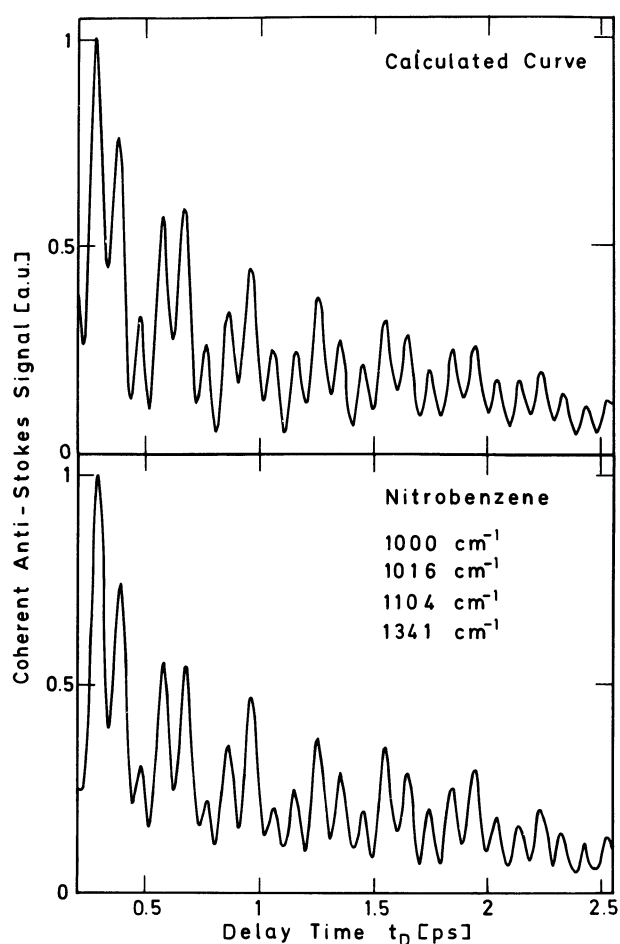


Fig. 6. — Time resolved coherent Raman data for liquid nitrobenzene. (a) The curve (calculated by a least square-fit procedure) should be compared with the results shown below). The four vibrational components with difference frequencies $\Delta\nu/c$ up to 340.8 cm^{-1} are listed in figure 6b. (b) Experimental curve of liquid nitrobenzene showing high-frequency beat phenomena extending to frequencies of 10.5 THz.

differences $\Delta\Omega$ may be determined with a precision approaching 10^{-3} .

5. Summary.

In this paper we have extended Fourier transform coherent Raman spectroscopy to the frequency range of 10 THz. With this technique we are now able to resolve terahertz phenomena with high accuracy.

Two points are relevant : (i) the frequency resolution is determined by the total time interval of the experiment. In order to improve spectral resolution the coherent signal has to be measured over delay times as long as possible. Taking into account the exponential decay of the signal with $T_2/2$ one immediately finds that the spectral resolution is directly related to the signal-to-noise ratio of the experiment. (ii) The duration of the exciting and

probing pulses does not influence the frequency resolution of the experiment, but determines the highest detectable beat frequencies to approximately

$\Delta\nu_{\max} \approx 1/t_p$. Under the present experimental conditions beat frequencies exceeding 10 THz are readily detected.

References

- [1] LAUBEREAU, A., KAISER, W., *Rev. Mod. Phys.* **50** (1978) 607 ;
PENZKOFER, A., LAUBEREAU, A., KAISER, W., *Progr. Quantum. Electron.* **6** (1979) 55.
- [2] VON DER LINDE, D., LAUBEREAU, A., KAISER, W., *Phys. Rev. Lett.* **26** (1971) 954.
- [3] VELSKO, S., TROUT, J., HOCHSTRASSER, R. M., *J. Chem. Phys.* **79** (1983) 2114.
- [4] GALE, G. M., GUYOT-SIONNEST, P., ZHENG, W. Q., *Opt. Commun.* **58** (1986) 395.
- [5] D'YAKOV, Yu. S., KRIKUNOV, S. A., MAGNITSKIL, S. A., NIKITIN, S. Yu., TUNKIN, V. G., *Sov. Phys. JETP* **57** (1983) 1172.
- [6] ZINTH, W., KAISER, W., *In Organic Molecular Aggregates*, Eds R. Reinecker, H. Haken, H. C. Wolf, Solid State Science, Vol. 49 (Springer, New York) 1983, p. 124.
- [7] GRAENER, H., LAUBEREAU, A., *Opt. Commun.* **54** (1985) 141.
- [8] ZINTH, W., *Opt. Commun.* **34** (1980) 479.
- [9] ZINTH, W., NUSS, M. C., KAISER, W., *Chem. Phys. Lett.* **88** (1982) 257.
- [10] COLLINS, M. A., MADDEN, P. A., BUCKINGHAM, A. D., *Chem. Phys.* **94** (1985) 291.
- [11] ZINTH, W., NUSS, M. C., KAISER, W., *Phys. Rev. A* **30** (1984) 1139.
- [12] LEONHARDT, R., HOLZAPFEL, W., ZINTH, W., KAISER, W., *Chem. Phys. Lett.* **133** (1987) 373.
- [13] ZINTH, W., LEONHARDT, R., HOLZAPFEL, W., KAISER, W., submitted to *J. Quantum Electron.*
- [14] CARMAN, R. L., SHIMIZU, I., WANG, C. S., BLOEMBERGEN, N., *Phys. Rev. A* **2** (1970) 60.
- [15] ZINTH, W., LAUBEREAU, A., KAISER, W., *Opt. Commun.* **26** (1978) 457.
- [16] NUSS, M. C., LEONHARDT, R., ZINTH, W., *Opt. Lett.* **10** (1985) 16.
- [17] DOBLER, J., SCHULZ, H. H., ZINTH, W., *Opt. Commun.* **57** (1986) 407.
- [18] LONG, D. A., MURFIN, F. S., THOMAS, E. L., *Trans. Farad. Soc.* **59** (1963) 12.
- [19] WIBERG, K. B., SHRAKE, A., *Spectrochim. Acta* **27A** (1971) 1139.
-